



Cite this: *Chem. Commun.*, 2021, 57, 3480

Received 16th February 2021,
Accepted 4th March 2021

DOI: 10.1039/d1cc00786f

rsc.li/chemcomm

Aptamer-based proximity labeling guides covalent RNA modification†

Daniel Englert,^a Regina Matveeva,^a Murat Sunbul,^{id}*^a Richard Wombacher*^{ab} and Andres Jäschke^{id}*^a

We describe the development of a proximity-induced bio-orthogonal inverse electron demand Diels–Alder reaction that exploits the high-affinity interaction between a dienophile-modified RhoBAST aptamer and its tetramethyl rhodamine methyltetrazine substrate. We applied this concept for covalent RNA labeling in proof-of-principle experiments.

The site-specific modification of biomolecules, *e.g.* with fluorescent dyes or crosslinkers, is an important yet exceedingly complex task. The limited number of different functional groups present in a given macromolecule represents a serious hurdle for achieving single-site selectivity. In the field of protein modification, one of the successful solutions to this problem utilizes proximity-enhanced reactivity.^{1–3} In these approaches, a high-affinity non-covalent interaction (*e.g.*, between an enzyme and its substrate) is used to position certain reactive groups of the two binding partners in close proximity to each other, thereby causing an increased reaction rate at these positions but not at others and allowing specific labeling. Here we transfer this concept to covalent RNA modification, using a high-affinity aptamer–dye interaction as the guiding principle.

Aside from a few ribozyme-based methods that directly attach the label,^{4–6} the majority of currently used covalent RNA labeling techniques are based on bio-orthogonal click reactions and require the initial introduction of a chemical handle to the RNA of interest (ROI) in the first step. The introduced functional group is subsequently derivatized *via* the corresponding click reaction. Based on the time point of incorporation of the reactive handle, these RNA labeling techniques can be classified into two categories: postsynthetic labeling strategies and the direct incorporation of modified nucleotides during

synthesis.⁷ The former approach repurposes methyl transferases^{8,9} or poly(A) polymerases,¹⁰ which modify the mRNA cap structure or the 3′-end, respectively. However, these methods are unspecific and label all RNAs in a sample, while sequence-specific labeling of an ROI has been accomplished using tRNA-modifying enzymes.^{11,12} The latter strategy uses the incorporation of the modified nucleotides during enzymatic synthesis.^{13,14} Applying this technique, various dienophiles were introduced into RNA and subsequently labeled *via* inverse electron demand Diels–Alder (IEDDA) reaction *in vitro*.^{15,16} An important advantage of enzymatic incorporation is its potential *in vivo* application in cells in the context of metabolic labeling. For this purpose, several different modified nucleoside analogues bearing ethynyl,¹⁷ azido¹⁸ or vinyl¹⁹ groups were synthesized and applied in mammalian cells. However, since the modified nucleoside triphosphate (NTP) is incorporated stochastically, it is impossible to control the site of modification, rendering this method unsuitable for specific labeling of a ROI.

Here, we report a solution to this problem by combining the ubiquitous incorporation of “clickable” nucleotides into an aptamer tag and a subsequent proximity-induced selective bio-orthogonal reaction. We use our recently developed fluorescent light-up aptamer RhoBAST and its fluorogenic target tetramethyl rhodamine dinitroaniline conjugate (**TMR-DN**) as a starting point²⁰ and exploit the high binding affinity and selectivity of the aptamer towards the 5-carboxy tetramethyl rhodamine (**TMR**) moiety to establish a proximity-induced reaction. Owing to the high selectivity of the IEDDA reaction *in vitro* and in cellular environment, we decided to enzymatically incorporate dienophile-modified nucleotides into the aptamer and use a **TMR-methyltetrazine** substrate (**TMR-Tz**) as a reactive diene (Fig. 1).²¹ Binding of **TMR-Tz** to the modified RhoBAST aptamer should lead to a close proximity of diene and dienophile and consequently to an enhanced reactivity in the IEDDA reaction.

We decided to introduce the required dienophile moiety on the C₅-position of uridine triphosphate (UTP), since a wide variety of UTP derivatives with C₅-modifications are known to be accepted by T7 RNA polymerase (T7 RNAP) and incorporated into RNA.^{13,15,22} Overall, we chose a set of four small and stable

^a Institute of Pharmacy and Molecular Biotechnology, Heidelberg University, Im Neuenheimer Feld 364, Heidelberg 69120, Germany.

E-mail: jaeschke@uni-hd.de, msunbul@uni-heidelberg.de
wombacher@uni-heidelberg.de

^b Department of Chemical Biology, Max Planck Institute for Medical Research, Jahnstrasse 29, Heidelberg 69120, Germany

† Electronic supplementary information (ESI) available. See DOI: 10.1039/d1cc00786f

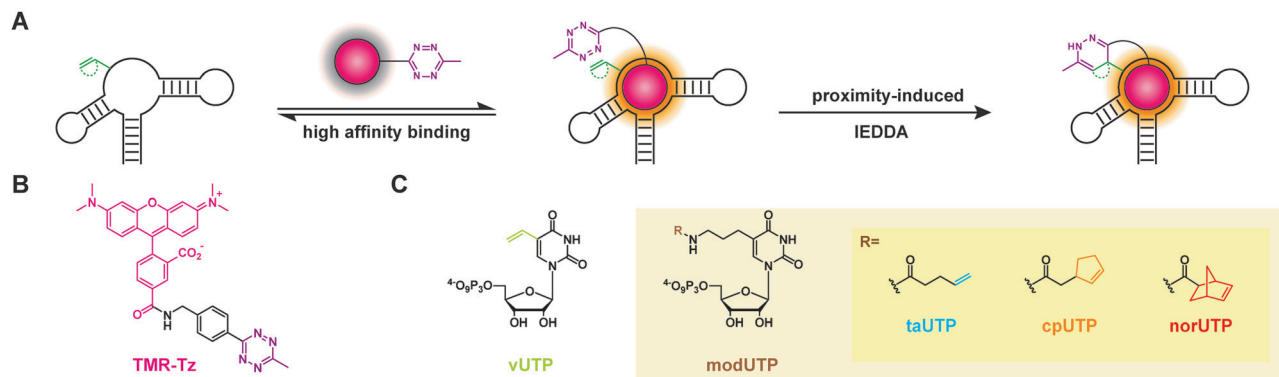


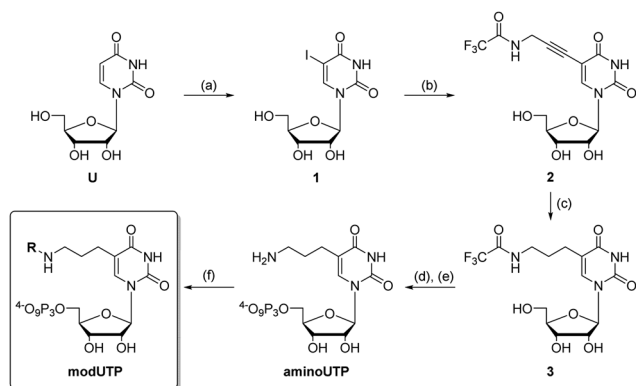
Fig. 1 Proximity-induced covalent RNA labeling. (A) Schematic illustration of the proximity-induced IEDDA reaction using a dienophile-modified RhoBAST aptamer and **TMR-Tz** substrate. Chemical structures of **TMR-Tz** (B) and the synthesized dienophile-substituted uridine triphosphates for enzymatic incorporation (C). Novel modified triphosphate derivatives (**modUTP**) are highlighted with a yellow box.

dienophiles with low-to-medium intrinsic reactivity (Fig. 1C). The reactivity of the dienophiles has to be low enough not to cause any unspecific reaction but high enough to be accelerated upon induced proximity to result in a specific labeling. Therefore, we prepared a vinyl-substituted **vUTP** derivative¹⁵ and three novel modified UTP derivatives bearing dienophile moieties with increasing ring strain and thus increasing reactivity in the IEDDA reaction (terminal alkene < cyclopentene < norbornene).^{21,23} All derivatives were synthesized starting from uridine, which in the first step was transferred to 5-iodo-uridine (**1**) by oxidative iodination (Scheme 1). Still cross-coupling with tributyl (vinyl)tin provided the vinyl-substituted uridine derivative **vU**, which was converted to its nucleoside triphosphate equivalent **vUTP** using a standard phosphorylation procedure.¹⁵ The novel modified uridine triphosphates **taUTP**, **cpUTP** and **norUTP** were prepared in 5 steps starting from **1** utilizing Sonogashira coupling with *N*-trifluoroacetyl propargyl amine. In order to increase the flexibility of the attached linker, the alkyne was hydrogenated using Adams' catalyst to yield **3**. In the next step, the modified nucleoside **3** was phosphorylated and deprotected to afford the precursor **aminoUTP**, bearing a primary amino group that enables late-stage

functionalization. In the final step, the different dienophile moieties were introduced by amide coupling using the corresponding organic acids as activated NHS-esters yielding the desired modified uridine triphosphates **taUTP**, **cpUTP** and **norUTP**.

Next, we tested the enzymatic incorporation of the modified UTPs in an *in vitro* transcription reaction using T7 RNAP, fully replacing UTP by the modified UTPs in the reaction mixture. As initial test, we transcribed the RhoBAST aptamer (55 nt), which contains 7 uridines, from a double-stranded DNA template. The obtained transcription mixtures were analyzed by denaturing polyacrylamide gel electrophoresis (PAGE). For all nucleotides, successful incorporation was observed and full-length RNA products were detected. As anticipated, the modified RNAs showed a slightly lower mobility in PAGE, compared to the unmodified transcription product (Fig. S1, ESI[†]). The transcription yield was determined by quantifying the ethidium bromide-stained full-length RNA product band. Reactions with the modified analogs **vUTP**, **taUTP** and **cpUTP** showed excellent transcription yields (>80%) relative to the control reaction using UTP. Even with the sterically demanding norbornene derivative **norUTP**, transcription yields >50% were achieved. The enzymatic incorporation of the modified UTPs was confirmed by LC-MS analysis of enzymatically digested PAGE-purified transcription products (Fig. S2, ESI[†]).

Subsequently, we tested if the commercial **TMR-Tz** substrate binds to the unmodified RhoBAST aptamer and if the introduced uridine modifications inhibit binding. As negative control, we designed an inactive version of the RhoBAST aptamer, also containing 7 uridines, by mutating essential and conserved regions (Fig. S3A, ESI[†]).²⁰ As expected, inactive RhoBAST did not increase the fluorescence of our previously developed turn-on probe **TMR-DN**,²⁴ confirming that inactive RhoBAST lost its affinity to **TMR** derivatives (Fig. S3B, ESI[†]). After incubation with **TMR-Tz**, we observed comparable fluorescence enhancement (~20-fold) for the unmodified RhoBAST aptamer and the modified aptamers with incorporated **vU**, **taU** or **cpU** (Fig. S3C, ESI[†]). Only the norbornene-modified version displayed a notably lower fluorescence enhancement (~12-fold turn-on). Regardless of the modification, the inactive control RNAs showed no significant



Scheme 1 Synthesis of novel modified uridine triphosphates (**modUTP**). (a) I_2 , HNO_3 , $CHCl_3$; (b) TFA-propargyl amine, $Pd(PPh_3)_4$, CuI , NEt_3 , DMF ; (c) H_2 , PtO_2 , $MeOH$; (d) $POCl_3$, proton sponge, TMP , $(n-Bu_3NH)_2H_2P_2O_7$, $n-Bu_3N$; (e) $NH_3(aq)$; (f) NHS-ester, $Na_2B_4O_7$ buffer, DMF .

turn-on. Furthermore, non-covalent complex formation between **TMR-Tz** and active aptamer was indicated by a bathochromic shift of the excitation and emission spectra of **TMR-Tz** (Fig. S4, ESI†). To further characterize the binding properties of the dienophile-modified RhoBAST aptamers, we determined their dissociation constants in complex with **TMR-Tz** (Fig. S5, ESI†). Introduction of C₅-modified uridines caused about one order of magnitude loss in binding affinity compared to the unmodified RhoBAST aptamer ($K_D = 5$ nM). We observed a trend between the sterical demand of the modification and the binding affinity: the aptamer with the smallest **vU** modification exhibited the strongest affinity ($K_D = 44$ nM) while the one with the bulky **norU** modification showed the weakest affinity ($K_D = 79$ nM).

We next examined if the RNA-appended dienophiles would still react in an IEDDA reaction. For this purpose, active and inactive RhoBAST RNAs (1 μ M) were incubated with an excess of **TMR-Tz** (5 μ M) for 20 hours. PAGE gel analysis of the labeling reactions revealed fluorescent bands with reduced mobility for all modified RNAs independent of the RNA sequence (Fig. S6, ESI†), confirming the IEDDA-reactivity of the modified RNAs. In contrast, no fluorescent reaction product was detected for the unmodified RhoBAST aptamer.

We then investigated if binding of the **TMR-Tz** substrate to the dienophile-modified aptamers induces an increase of the reaction rate. Thus, we compared the reaction kinetics of the active and inactive RhoBAST aptamers using an equimolar concentration (1 μ M) of **TMR-Tz** (Fig. 2A and Fig. S7, ESI†). For the reaction of the inactive RhoBAST samples, the expected reactivity trend was observed: the RNAs modified with vinyl (**vU**) and the terminal alkene (**taU**) displayed the lowest IEDDA rate, whereas RNAs with incorporated cyclic dienophiles (**cpU** and **norU**) reacted faster. Overall, the reaction rate increased with ring strain (**vU** \sim **taU** < **cpU** << **norU**). Importantly, a different reactivity pattern was observed for the modified active RhoBAST aptamers. The active **taU** and **cpU** aptamers showed IEDDA rates similar to their inactive counterparts, implying the absence of proximity effect. In contrast, remarkably higher rates were measured for the active **vU** and **norU** RhoBAST aptamers, compared to their inactive mutants, indicating a proximity-induced reactivity enhancement caused by binding of **TMR-Tz** to the dienophile-modified RhoBAST aptamers. The active **norU** RhoBAST aptamer showed the highest reaction rate, but only a two-fold

enhancement over the inactive **norU** aptamer. Comparing the active to the inactive **vU**-RhoBAST aptamer, a more than 30-fold higher IEDDA rate for the proximity-induced reaction (Fig. S8, ESI†) and a labeling yield of 10% after 24 h (Fig. S9, ESI†) could be observed. Based on these results, we focused on the **vU**-modified RNAs for further experiments. Investigation of the initial rate of the IEDDA reaction as a function of the **TMR-Tz** substrate concentration revealed for active **vU**-RhoBAST a saturation-type curve reminiscent of the Michaelis–Menten plots of enzyme-catalyzed reactions, indicating the formation of an aptamer–substrate complex at equilibrium, followed by the rate-determining chemical step, the IEDDA reaction (Fig. S10, ESI†). In contrast, inactive **vU**-RhoBAST showed a linear concentration–rate profile, as expected for a second-order reaction without proximity effects (Fig. S11, ESI†). This difference in the reaction kinetics means that at high **TMR-Tz** concentrations the highest rates but the lowest selectivities are achieved. Conversely, low substrate concentrations allow highly specific modification, albeit at a low rate. Mutation analysis indicated uridine U39 as the major site of the IEDDA reaction (Fig. S12, ESI†).

To further support the conclusion that the increased IEDDA rate of active **vU**-RhoBAST RNA is based on induced proximity, we performed an experiment in which the formation of the RhoBAST***TMR-Tz** complex was challenged by a competitor. For this purpose, we used **TMR**, a known high-affinity binder of RhoBAST, in 1000-fold excess over **TMR-Tz**.^{20,24} As expected, the addition of **TMR** to the proximity-induced reaction resulted in a dramatic drop of reaction product to roughly the level observed for the inactive mutant (Fig. 2B). Addition of **TMR** to the IEDDA reaction of the inactive RhoBAST mutant, on the other hand, had no influence on the reaction yield. The IEDDA reaction of **vU**-RhoBAST was additionally performed with 1 μ M of tetrazine-modified fluorescein (**FAM-Tz**) and cyanine (**Cy5-Tz**) dyes that are not expected to bind RhoBAST (Fig. S13A, ESI†).²⁴ Only the combination of **vU**-RhoBAST aptamer and **TMR-Tz** resulted in a significantly increased product formation of active vs. inactive aptamer, further substantiating the importance of aptamer–substrate complex formation. Using higher concentrations (100 μ M) of **FAM-Tz** and **Cy5-Tz** resulted in unspecific multiple labeling of **vU**-modified RNAs (Fig. S13B, ESI†).

To demonstrate the specificity of our proximity-based IEDDA system, we treated a mixture of different *in vitro* transcribed **vU**-modified RNAs with **TMR-Tz**. RhoBAST (55 nt), an inactive RhoBAST mutant with an elongated stem (67 nt), and an unrelated 39 mer (1 μ M each) were mixed and treated with **TMR-Tz** (1 μ M). Analysis of the reaction products showed that only the RhoBAST RNA was significantly labeled with **TMR-Tz** and hence confirmed the expected selectivity of the proximity-induced reaction (Fig. 3A). As a control, all modified RNAs were labeled unspecifically using high concentrations of **Cy5-Tz** (5 μ M). Encouraged by these *in vitro* results, we aimed to apply our proximity-induced covalent IEDDA approach to RNAs transcribed inside living cells by combining it with metabolic labeling. **vU** is known to be taken up from the medium, metabolically converted to **vUTP**, and incorporated into cellular RNAs, although the incorporation efficiency appears to be

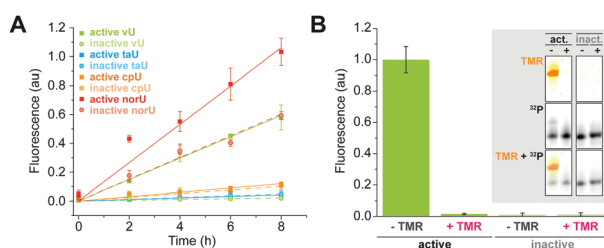


Fig. 2 IEDDA reaction of modified active and inactive RhoBAST aptamers. (A) Kinetics of IEDDA reactions with equimolar concentrations of RNA and **TMR-Tz** (1 μ M) at 37 $^{\circ}$ C. (B) Yield of the IEDDA reaction (37 $^{\circ}$ C, 20 h) of **vU**-modified RhoBAST RNAs (1 μ M) with **TMR-Tz** (1 μ M) in the presence or absence of excess competitor **TMR** (1 mM).

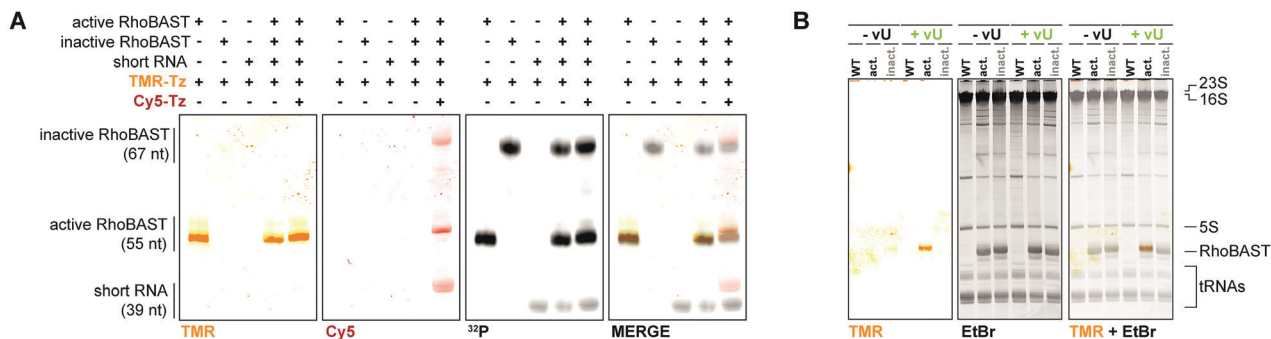


Fig. 3 Covalent labeling of **vU**-RhoBAST in RNA mixtures. (A) Denaturing PAGE gel (20%) analysis of individual and one-pot labeling of **vU**-modified active (55 nt) and inactive (elongated version, 67 nt) RhoBAST and **vU**-modified 39 mer (1 μ M each) with **TMR-Tz** (1 μ M) and **Cy5-Tz** (5 μ M). (B) PAGE gel (10%) analysis of labeling reactions of total RNA isolated from *E. coli* transcribing active and inactive RhoBAST aptamers. Bacteria were grown in the presence or absence of **vU** (2 mM). IEDDA reactions were performed using 50 μ M **TMR-Tz** and 4 μ g μ L⁻¹ total RNA at 37 °C for 20 h (10 μ g sample per lane).

rather low.¹⁹ Here, we cloned active and inactive RhoBAST aptamers into a pET vector and transformed them into *E. coli* BL21 (DE3). Then, the *E. coli* strains were grown in the presence and absence of **vU** (2 mM), and total RNA was isolated. After refolding of the RNA, we incubated the samples with **TMR-Tz** and performed PAGE analysis using in-gel fluorescence and EtBr staining (Fig. 3B). For total RNA samples extracted from *E. coli* growing in the absence of **vU** (negative control), no fluorescent signal was observed, whereas in the isolated RNA samples from *E. coli* growing in presence of **vU**, only one distinct band was detected for the sample containing the active RhoBAST aptamers. This fluorescent band showed the same mobility on the PAGE gel as the *in vivo* transcribed and ethidium bromide stained RhoBAST. In contrast, no signal was detected for the inactive RhoBAST sample, demonstrating the specific labeling of RhoBAST in *in vivo* transcribed complex RNA mixtures.

In conclusion, we described the first application of *in vitro* selected RNA aptamers to increase the reaction rate of a biorthogonal IEDDA reaction by proximity effects. We could clearly demonstrate that the over 30-fold reactivity increase is due to the specific interaction between aptamer and target. This novel principle enabled us to specifically label an *in vitro* or *in vivo* transcribed ROI in a mixture of modified RNAs. However, for wide-spread practical application as a covalent labeling tool the reaction rate must be increased significantly without sacrificing selectivity.

Open Access funding provided by the Max Planck Society.

Conflicts of interest

There are no conflicts to declare.

Notes and references

- 1 S. Tsukiji, M. Miyagawa, Y. Takaoka, T. Tamura and I. Hamachi, *Nat. Chem. Biol.*, 2009, 5, 341–343.

- 2 S. S. Gallagher, J. E. Sable, M. P. Sheetz and V. W. Cornish, *ACS Chem. Biol.*, 2009, 4, 547–556.
- 3 M. Sunbul, L. Nacheva and A. Jäschke, *Bioconjugate Chem.*, 2015, 26, 1466–1469.
- 4 M. Ghaem Maghami, C. P. M. Scheitl and C. Höbartner, *J. Am. Chem. Soc.*, 2019, 141, 19546–19549.
- 5 R. I. McDonald, J. P. Guilingher, S. Mukherji, E. A. Curtis, W. I. Lee and D. R. Liu, *Nat. Chem. Biol.*, 2014, 10, 1049.
- 6 A. K. Sharma, J. J. Plant, A. E. Rangel, K. N. Meek, A. J. Anamisis, J. Hollien and J. M. Heemstra, *ACS Chem. Biol.*, 2014, 9, 1680–1684.
- 7 D. Schulz and A. Rentmeister, *ChemBioChem*, 2014, 15, 2342–2347.
- 8 J. M. Holstein, D. Schulz and A. Rentmeister, *Chem. Commun.*, 2014, 50, 4478–4481.
- 9 J. M. Holstein, D. Stummer and A. Rentmeister, *Chem. Sci.*, 2015, 6, 1362–1369.
- 10 M.-L. Winz, A. Samanta, D. Benzinger and A. Jäschke, *Nucleic Acids Res.*, 2012, 40, e78.
- 11 F. Li, J. Dong, X. Hu, W. Gong, J. Li, J. Shen, H. Tian and J. Wang, *Angew. Chem., Int. Ed.*, 2015, 54, 4597–4602.
- 12 S. C. Alexander, K. N. Busby, C. M. Cole, C. Y. Zhou and N. K. Devaraj, *J. Am. Chem. Soc.*, 2015, 137, 12756–12759.
- 13 J. D. Vaught, T. Dewey and B. E. Eaton, *J. Am. Chem. Soc.*, 2004, 126, 11231–11237.
- 14 N. Milisavljević, P. Perliková, R. Pohl and M. Hocek, *Org. Biomol. Chem.*, 2018, 16, 5800–5807.
- 15 J. T. George and S. G. Srivatsan, *Bioconjugate Chem.*, 2017, 28, 1529–1536.
- 16 P. Asare-Okai, E. Agustin, D. Fabris and M. Royzen, *Chem. Commun.*, 2014, 50, 7844–7847.
- 17 C. Y. Jao and A. Salic, *Proc. Natl. Acad. Sci. U. S. A.*, 2008, 105, 15779–15784.
- 18 S. Nainar, S. Beasley, M. Fazio, M. Kubota, N. Dai, I. R. Corrèa Jr and R. C. Spitale, *ChemBioChem*, 2016, 17, 2149–2152.
- 19 M. Kubota, S. Nainar, S. M. Parker, W. England, F. Furche and R. C. Spitale, *ACS Chem. Biol.*, 2019, 14, 1698–1707.
- 20 M. Sunbul, J. Lackner, A. Martin, D. Englert, B. Hacene, F. Grün, K. Nienhaus, G. U. Nienhaus and A. Jäschke, *Nat. Biotechnol.*, 2021, DOI: 10.1038/s41587-020-00794-3.
- 21 B. Oliveira, Z. Guo and G. Bernardes, *Chem. Soc. Rev.*, 2017, 46, 4895–4950.
- 22 M. Flamme, L. K. McKenzie, I. Sarac and M. Hollenstein, *Methods*, 2019, 161, 64–82.
- 23 P. Werther, J. S. Möhler and R. Wombacher, *Chem. – Eur. J.*, 2017, 23, 18216–18224.
- 24 M. Sunbul and A. Jäschke, *Nucleic Acids Res.*, 2018, 46, e110.